FAST APPROXIMATIONS OF THE ORTHOGONAL DUAL-TREE WAVELET BASES

Adeel Abbas and Trac D. Tran

Department of Electrical and Computer Engineering,
The Johns Hopkins University, Baltimore, MD 21218
E-mail: adeel@jhu.edu, trac@jhu.edu

ABSTRACT

Recently, there has been a significant interest in the design of iterated filter banks in which the resulting wavelet bases form an approximate Hilbert transform pair. In this work, we propose three approximations of such dual-tree wavelet bases that satisfy Hilbert transform conditions. Our designs are derived from Selesnick's and Kingsbury's orthogonal wavelet filter solutions, and meet other desirable properties such as high coding gain, reduced computational complexity and sufficient regularity. The Quantization is performed in lattice domain using sum-of-power-of-two (SOPOT) coefficients. Several performance comparisons are presented. Furthermore, this paper introduces a proposition that lattice coefficients of filters that are time-reversals of each other are closely related.

1. INTRODUCTION

The discrete wavelet transform (DWT) offers solutions in a wide variety of image and signal processing applications, including compression, denoising, classification, and many others. The last couple of years have seen significant progress in the theory and design of M-channel filter banks and wavelets [1]. However, there are well known limitations in the conventional wavelet design, for example the lack of directionality/phase information and poor shift invariance. The aim of research in the field of complex wavelet transforms is to explore solutions to these limitations, while benefiting from the existing advantages that wavelets provide.

Several authors have proposed that in a formulation where two dyadic wavelet bases form a Hilbert transform pair, DWT can provide answer to some of the aforementioned limitations. Shown in Fig. 1, Kinsbury's complex dual-tree [2] has received considerable interest. In dual-tree, two real wavelet trees are used, each capable of perfect reconstruction (PR). One tree generates the real part of the transform and the other is used in generating complex part. As shown, $\{H_0(z), H_1(z)\}$ is a Quadrature Mirror Filter (QMF) pair in the real-coefficient analysis branch. For the complex part, $\{G_0(z), G_1(z)\}$ is another QMF pair in the anaylsis branch. All filter pairs discussed here are orthogonal, real-valued and are power-complementary.

It has been shown [3] that if filters in both trees can be made to be offset by half-sample, two wavelets satisfy Hilbert transform pair condition. Thus if

$$G_0(\omega) \simeq H_0(\omega) \times e^{-j\theta(\omega)} \quad \theta(\omega) \simeq \omega/2$$

Then

$$\psi_g(\omega) \simeq \begin{cases} -j\psi_h(\omega) & \omega > 0 \\ j\psi_h(\omega) & \omega < 0 \end{cases}.$$

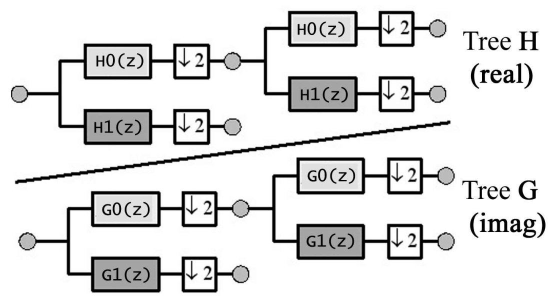

Fig. 1. Kingsbury's dual tree DWT.

2. DESIGN PROCEDURE

Our design procedure is governed by global optimization of the following parameters:

- Coding Gain relates to the ability of a sub-band coder to compress most of the signal energy in least number of bands. The biorthogonal coding gain $\mathbf{C}_g$ is defined as:

$$\mathbf{C}_g = 10 \times \log_{10} \frac{\sigma_x^2}{\left(\prod_{i=0}^{M-1} \sigma_{xi}^2 \times \|f_i\|^2\right)^{1/M}}$$

Where:

This work is partially supported by NSF CAREER CCF-0093262 and NSF CCF-0430869

M	Number of sub-bands
σ_x^2	Variance of input
σ_{xi}^2	Variance of i-th sub-band
$\parallel f_i \parallel^2$	L-2 norm of i-th synthesis basis function

Where input is a first order Gaussian-Markov process with zero-mean, unit variance and correlation coefficient 0.95.

- Hilbert Transform characteristics are related to the directional selectivity of the dual-tree DWT. Thus, the frequency response of the function $\psi_h[n]+j\psi_g[n]$ should have high attenuation for all frequencies in the region $-\infty < \omega < 0$. In order to measure this, we propose a new measure, Hilbert PSNR (HPSNR), defined as

$$HPSNR \;=\; 10 \times \log_{10}\left(\frac{max|\psi_h(\omega)+j\psi_g(\omega)|^2}{\int_{-\infty}^{0}|\psi_h(\omega)+j\psi_g(\omega)|^2\,d\omega}\right).$$

- DC Leakage or Vanishing Moments (DCPSNR) is another property that distinguishes wavelets from classical filter banks. It is defined as the number of zeros of the low-pass filters at $Z=-1$ and is directly related to the smoothness of the resulting wavelet and scaling functions. After quantization, the zeros at $Z=-1$ get perturbed, however by enforcing that the sum of all the lattice angles, θ_i satisfies

$$\sum_i \theta_i = \{\pi/4, 5\pi/4\} \pm 2\pi k,$$

we can still fix one zero to be at exactly $Z=-1$. This would imply that no DC should be picked up in the high-pass sub-band. It would also enforce $\sum_n h_1[n]=0$ where $h_1[n]$ is the analysis high-pass filter.

We used the software Singular[1] to develop a framework to switch from filter domain to lattice domain and perform heuristic search amongst several solutions. Smoother wavelets are needed for $H_0(z)$, because it is intended for compression applications. Therfore the quantization bits for $H_0(z)$ are selected so that coding gain is maximized. Since $G_0(z)$ is used only when Hilbert transform is required, its smoothness is not critical. For two out of three designs presented here, $G_0(z)$ is approximated accordingly to maximize its Hilbert characteristics, yet maintaining its applicability in traditional signal processing operations.

2.1. Design Via Exhaustive Search

Our first design is termed Lat-6 and it is obtained by exhaustive search in three Lattice stages. This design is based on Kingsbury's Q-shift scheme, so the filter set $\{G_0(z), G_1(z)\}$ is taken to be a time-reversal of $\{H_0(z), H_1(z)\}$. As will be explained soon, under this condition, the lattice coefficients of $\{G_0(z), G_1(z)\}$ can be directly derived from those of $\{H_0(z), H_1(z)\}$. The DC leakage condition introduced above allows us to express one of the angles in terms of the other two. Thus, the optimization problem reduces to a search in 2-D space. Results from this search are plotted in

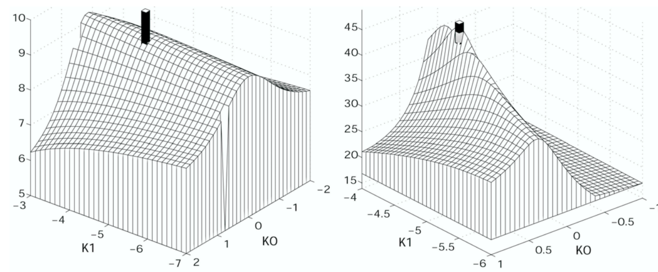

Fig. 2. Exhaustive search results, in dB, for Coding Gain (left) and Hilbert PSNR (right). The black cylinders mark the point that corresponds to Lat-6 implementation.

3D (in Fig. 2) against first two lattice coefficients (K_0 and K_1). It is clear that the Hilbert performance of this design is optimal for a 3-lattice structure. The polyphase factorization of this implementation is as follows:

$$\mathbf{H}_p(z) = \begin{bmatrix} -5/64 & 0 \\ 0 & -5/64 \end{bmatrix} \begin{bmatrix} 1 & 3/16 \\ -3/16z^{-1} & z^{-1} \end{bmatrix} \cdots \times \begin{bmatrix} 1 & -37/8 \\ 37/8z^{-1} & z^{-1} \end{bmatrix} \begin{bmatrix} 1 & -5/2 \\ 5/2z^{-1} & z^{-1} \end{bmatrix}$$

$$\mathbf{G}_p(z) = \begin{bmatrix} -1/64 & 0 \\ 0 & -1/64 \end{bmatrix} \begin{bmatrix} 1 & 85/16 \\ -85/16z^{-1} & z^{-1} \end{bmatrix} \cdots \times \begin{bmatrix} 1 & 37/8 \\ -37/8z^{-1} & z^{-1} \end{bmatrix} \begin{bmatrix} 1 & 5/2 \\ -5/2z^{-1} & z^{-1} \end{bmatrix}.$$

The filter coefficients for this design are shown in Table 3.

2.2. Design Via Approximation

The next design, called Lat-12, is based on Selesnick's approach in [3] (called Sel-12) where the author described a systematic design procedure based on spectral factorization. In this procedure, a flat-delay all-pass filter is used to approximate half sample delay between $H_0(z)$ and $G_0(z)$. The problem reduces to the design of only two filters: $H_0(z)$ and $G_0(z)$. Presented as Example 1A in [3], the two filters have 12-taps with 4 vanishing moments and 2rd order all-pass characteristics. As shown in Table 1, the dyadic rationals of Lat-12 are very good approximations of the irrationals originally proposed by Selesnick. The filter coefficients for this design are displayed in Table 3.

[1]Algebraic Geometry Group, Univ. of Kaiserslautern, Germany - http://www.singular.uni-kl.de/

Table 1. Selesnick's lattice and Lat-12 approximations

	$H_0(z)$ Coefficients		$G_0(z)$ Coefficients	
	Sel-12	Lat-12	Sel-12	Lat-12
κ_0	-7.48299980	$-31/4$	0.51739997	$1/2$
κ_1	-2.31345916	$-9/4$	7.54474640	$15/2$
κ_2	-2.40704036	$-5/2$	-0.25932312	$-1/4$
κ_3	1.75770926	$7/4$	-3.55918646	$-7/2$
κ_4	3.28926611	$13/4$	-2.48548698	$-5/2$
κ_5	-1.27999997	$-5/4$	-32.0000000	-25

2.3. Design Via the Time-Reversal Theorem

$Theorem$: For Kingsbury's Q-shift designs [2], the filter pair $\{G_0(z), G_1(z)\}$ is related to $\{H_0(z), H_1(z)\}$ by a time reversal. Let K_0, K_1, $\ldots$ K_{N-2}, K_{N-1} be lattice coefficients that implement $\{H_0(z), H_1(z)\}$ pair, where K_{N-1} is associated with the last rotation. Then, the lattice coefficients required to implement $\{G_0(z), G_1(z)\}$ pair will be $-K_0$, $-K_1$, $\ldots$ $-K_{N-2}$, $1/K_{N-1}$. Thus, inverting last coefficient and multiplying rest of the rotations by -1 implements the time-reversed filters. The proof is beyond the scope of this paper, but will be reported soon.

The final approximation is based on the above-mentioned theorem. Termed as Lat-14, it is based on a 14-tap Q-shift filter design proposed by Kingsbury (called Kings-14)[2]. In this case, the filter $G_0(z)$ is a time-reverse version of $H_0(z)$, and therefore is same as the low-pass filter in the real-synthesis branch. Lattice coefficients and quantized lattice are displayed in Table 2. The time reversal theorem is also evident from observing unquantized coefficients in Table 2, where product of the K_6 coefficients for $H_0(z)$ and $G_0(z)$ is one. For $K_0 \ldots K_5$, rotations have opposite sign but same magnitude. Implementation of Lat-14 is shown in Fig. 6.

Table 2. Kingsbury's lattice and Lat-14 approximations

	H_0 Coefficients		G_0 Coefficients	
	Kings-14	Lat-14	Kings-14	Lat-14
κ_0	-1.19400000	$-19/16$	1.19400000	$19/16$
κ_1	0.31583467	$5/16$	-0.31583467	$-5/16$
κ_2	12.6443805	$25/2$	-12.6443805	$-25/2$
κ_3	0.03376979	$1/16$	-0.03376979	$-1/16$
κ_4	-0.75500833	$-3/4$	0.75500833	$3/4$
κ_5	6.80293321	$21/4$	-6.80293321	$-21/4$
κ_6	-1.40100002	$-11/8$	-0.71377586	$-8/11$

3. EVALUATIONS AND APPLICATIONS

In this section, we define some of the figures of merit that will be used in evaluating the performance of the proposed designs.

3.1. Performance on JPEG-2000

For better compression, the wavelet and scaling functions should be as smooth as possible. Generally, this smoothness

[2]Matlab files for generating these filters are available at: http://www-sigproc.eng.cam.ac.uk/~ngk/

Table 3. Quantized filter coefficients

	Lat-12		Lat-6	
n	$h_0[n]$	$g_0[n]$	$h_0[n]$	$h_1[n]$
1	$-1/2^0$	$-1/2^0$	$-1/2^0$	$-1/2^0$
2	$31/2^2$	$-1/2^1$	$5/2^1$	$-5/2^1$
3	$325/2^4$	$74/2^0$	$1369/2^7$	$4625/2^7$
4	$-641/2^5$	$221/2^3$	$1739/2^8$	$14541/2^8$
5	$3349/2^7$	$-2077/2^4$	$-15/2^5$	$425/2^5$
6	$167787/2^9$	$39141/2^8$	$-3/2^4$	$-85/2^4$
7	$894613/2^{11}$	$107133/2^8$	–	–
8	$121285/2^{10}$	$18121/2^4$	–	–
9	$-22933/2^8$	$-735/2^3$	–	–
10	$-1079/2^5$	$-285/2^0$	–	–
11	$155/2^4$	$-25/2^1$	–	–
12	$5/2^2$	$25/2^0$	–	–
K	0.0017593	0.0004676	-0.0771427	-0.0145190

is directly related to the number of zeros at $Z = -1$. The integer-coefficient designs presented here generate functions that have accepetable smoothness and are very close approximations with low complexity. In Fig. 3 the Lat-12 wavelet and scaling functions (for analysis stage) are plotted. The Lat-12 designs are orthogonal, so the synthesis scaling and wavelet functions are the time-reversals of analysis functions. Some other factors worth considering are coding gain and DC leakage (results shown in Table 5).

The proposed families of wavelet filters have been implemented in JPEG-2000 compression engine. Table 4 compares PSNR results of integer-coefficient filters with popular Daubechies filters and the original Selesnick/Kingsbury designs. Only $H_0(z)$ is considered because the idea is to use only one of the trees in case compression is the ultimate goal. In summary, the performance of quantized filters is comparable to that of the Daubechies' filters and the previously published irrational-coefficient dual-tree CWT filters.

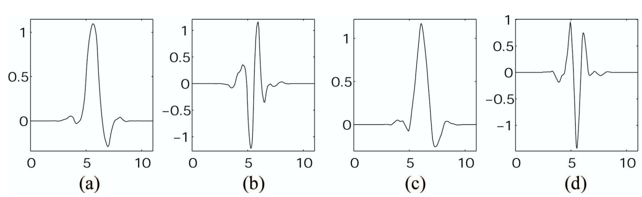

Fig. 3. Lat-12: (a) $\phi_h[n]$ (b) $\psi_h[n]$ (c) $\phi_g[n]$ (b) $\psi_g[n]$

3.2. Hilbert Performance and Directional 2-D Wavelets

Fig. 4 plots the function $|\psi_h(\omega) + j\psi_g(\omega)|$ for Lat-12 filters. We have found that the Hilbert performance of all of the proposed designs is as good as the original ones. Measurements of Hilbert PSNR are tabulated in Table 5.

3.3. Denoising performance

Due to shift-invariance and good directional selectivity, the dual-tree complex wavelet transform has been shown to be

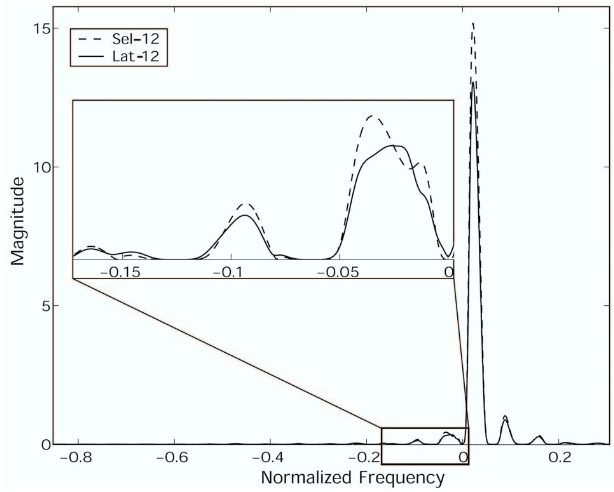

Fig. 4. Plot of function $|\psi_h(\omega) + j\psi_g(\omega)|$ for Lat-12.

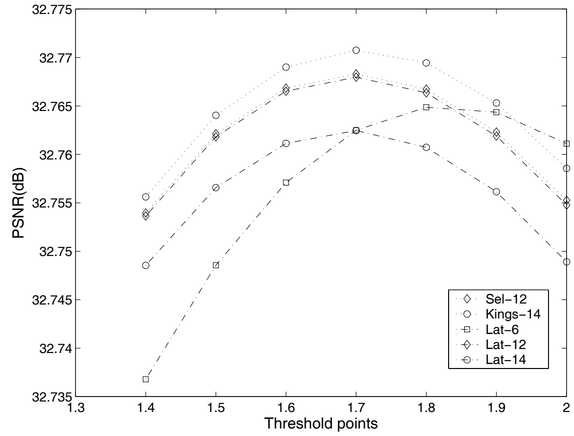

Fig. 5. PSNR Vs Threshold points plot. The image for this example had 32.22dB PSNR before denoising. The best achievable PSNR with separable 2-D DWT was 32.70dB.

Table 4. JPEG-2000 performance on standard test images

	Bitrate	Daub 9/7	Sel-12	Lat-12	Kings-14	Lat-14
Lena	0.5	37.22	37.05	37.01	37.00	36.57
	0.25	34.04	33.80	33.79	33.86	33.47
	0.125	30.65	30.43	30.26	30.45	30.24
Barb	0.5	32.30	32.26	32.19	32.54	32.40
	0.25	28.41	28.39	28.37	28.53	28.51
	0.125	25.26	25.35	25.37	25.51	25.48
Boat	0.5	34.64	34.48	34.47	34.38	34.14
	0.25	31.06	30.79	30.82	30.85	30.71
	0.125	28.01	27.94	27.89	27.99	27.82

Table 5. Property comparisons of the proposed designs

	Coding Gain (dB)				HPSNR (dB)	DCPSNR (dB)	
Filters	H_0	F_0	G_0	P_0		H_0	G_0
Lat-6	9.10	9.10	9.11	9.11	44.75	68.42	68.92
Sel-12	9.62	9.62	9.62	9.62	46.64	188.1	214.8
Lat-12	9.61	9.61	9.62	9.62	49.29	75.66	79.67
Kings-14	9.67	9.67	9.67	9.67	48.93	108.4	108.4
Lat-14	9.64	9.64	9.64	9.64	40.05	72.34	72.34

an effective tool for image and video denoising. An alternate argument to explain it is that CWT has bases functions that can capture edges in more number of orientations than real DWT. Thus, for CWT, edges at $\pm 15°$ and $\pm 75°$ are much better preserved after thresholding. Fig. 5 shows[3] PSNR Vs Threshold point plot for the stonehenge image.

4. CONCLUSION

We have presented efficient designs of Hilbert transform pairs of orthogonal wavelet bases. Lat-12 approximation is the best because of its high coding gain, better Hilbert characteristics and lower complexity. For compression, the real tree can be used alone. However, when the need is to obtain directional information, $G_0(z)$ can be applied to the same data. Furthermore, all of our filter coefficients are dyadic rationals, and as a result the designs can be mapped onto very efficient VLSI implementation.

[3]Most of our denoising experiments were based on the Matlab code available at http://taco.poly.edu/WaveletSoftware/index.html

5. REFERENCES

[1] P.P. Vaidyanathan, *Multirate Systems and Filter Banks*, Prentice Hall, 1992.

[2] N. G. Kingsbury, "The dual-tree complex wavelet transform: a new technique for shift invariance and directional filters," *IEEE DSP Workshop 98*, Aug. 1998.

[3] I. W. Selesnick, "The design of approximate hilbert transform pairs of wavelet bases," *IEEE Trans. on Signal Processing*, vol. 50, pp. 1144–1152, May 2002.

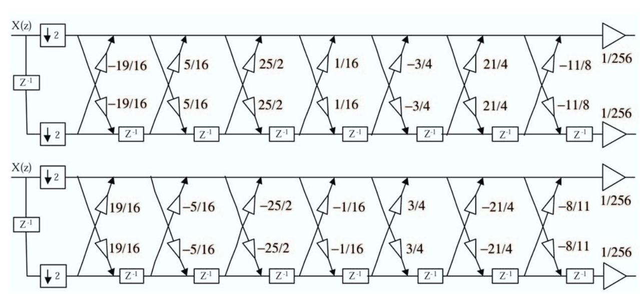

Fig. 6. Lattice-Domain Implementation of the Lat-14. Top: $\{H_0(z), H_1(z)\}$ Bottom: $\{G_0(z), G_1(z)\}$.